



## Characterization of Enhanced Antibacterial Effects of Silver Loaded Cerium oxide Catalyst

GUSLIANI EKA PUTRI<sup>1\*</sup>, SYUKRI ARIEF<sup>2</sup>, NOVESAR JAMARUN<sup>2</sup>,  
FENI RAHAYU GUSTI<sup>1</sup> and ANNISA NOVITA SARY<sup>1</sup>

<sup>1</sup>Sekolah Tinggi Ilmu Kesehatan Syedza Saintika, Padang, West Sumatera, Indonesia.

<sup>2</sup>Department of Chemistry, Faculty of Mathematic and Natural Sciences, Universitas Andalas, Indonesia.

\*Corresponding author E-mail: guslianiekaputri@gmail.com

<http://dx.doi.org/10.13005/ojc/340629>

Received: September 28, 2018; Accepted: November 10, 2018)

### ABSTRACT

Silver-cerium nanoparticles had been successfully synthesized using the sol-gel method by silver nitrate as a source of silver and cerium nitrate hexahydrate as a source of cerium. The synthesized silver-cerium nanoparticles had been characterized by X-ray diffraction, transmission electron microscopy, and scanning electron microscopy-energy dispersive X-ray. Based on the results of XRD and TEM analysis showed silver-cerium nanoparticles were spherical with the dominant size range of 8.9-12.73 nm. SEM-EDX analysis showed silver nanoparticles covered by cerium nanoparticles that were known as the core-shell structure. Silver nanoparticles doped with cerium nanoparticles (CeONP) showed an increase in inhibitory with an increase a zone of inhibition after being doped with cerium nanoparticles. The disinfection effect of Ag-doped CeONP was more pronounced on *Staphylococcus aureus* than *Escherichia coli*, although the difference was not wide.

**Keywords:** Cerium nanoparticles, Silver nanoparticles, Antimicrobacterial activity, Synthesis.

### INTRODUCTION

Cerium oxide was a material that has been widely researched lately because it has the ability to store oxygen so that it was possible to function as an oxygen storage in chemical catalytic processes<sup>1,2</sup>. Cerium oxide buffer function can occur because cerium has two oxidation numbers namely trivalent Ce<sup>3+</sup> and Ce<sup>4+</sup> tetravalent. Therefore, cerium oxide acts as an oxygen provider under an oxygen-deprived environment. After the oxide surface gives oxygen, Ce<sup>4+</sup> was reduced to Ce<sup>3+</sup> because the extra electrons are left behind<sup>3,4</sup>.

When the oxide surface lacks oxygen, Ce<sup>3+</sup> will tend to receive oxygen again. Cerium oxide nanoparticles have the ability to inactivate hydroxyl radicals of superoxide radicals, nitric oxide, and hydrogen peroxide<sup>5,6</sup>. Another urgent problem of the health care system was the growing resistance that bacteria develop very quickly. Various methods were used to create organic antibacterial agents that can quickly kill bacteria. Among the antibacterial agents that are the current conversation was cerium oxide<sup>7</sup>. Cerium oxide had a fast evolution rate. Cerium oxide provides a different mechanism



for killing bacteria or limiting bacterial cell growth<sup>8</sup>. Cerium oxide nanoparticles (CeONP) toxicity was associated with its properties as a reducing agent and killing bacteria by attacking membranes. Both mechanisms require direct contact with the cell wall and the spread of nanoparticles into bacteria so that it kills and weakens bacteria<sup>7,9</sup>. So that the antibacterial properties of cerium oxide were better than doped with silver nanoparticles. In principle, the degradation of bacteria and viruses by silver ions was that silver particles will damage and penetrate the bacterial cell wall, then enter the bacterial thiol group and bind to sulfhydryl groups in bacteria so as to prevent the production of enzymes in bacteria. Furthermore, silver particles will inhibit DNA growth and eventually bacteria die<sup>10</sup>. When applied as an antibacterial, it shown that CeONP was fed with silver not only releases silver ions but also increases the oxygen vacuum on the oxide surface. Thus, silver dopants introduce the Ag disinfection effect, which has been reported to be effective against several bacteria<sup>11,12</sup>.

In this reserach, we synthesized silver-cerium doped particles with nanometer size with a cost-effective sol-gel method and produced good quality particles. The resulting nanoparticles were used to inhibit the growth of *Escherichia coli* and *Staphylococcus aureus* bacteria.

## EXPERIMENTAL

### Chemicals and reagents

Cerium (III) nitrate hexahydrate ( $\text{Ce}(\text{NO}_3)_3 \cdot 6\text{H}_2\text{O}$ ) used for a precursor of  $\text{CeO}_2$ , acetic acid, ammonia solution, 2-propanol, silver nitrate, polyvinyl alcohol (PVA), glucose was purchase from Merck & Co. Synthesis of silver-cerium nanoparticles.

The source of the Ce metal was  $\text{Ce}(\text{NO}_3)_3 \cdot 6\text{H}_2\text{O}$  (cerium nitrate hexahydrate). Synthesis of cerium oxide (ceria) was done by making two solutions. The first solution was made by cerium nitrate hexahydrate dissolved in a mixture of a solvent of water and isopropanol with a ratio of 1:6. The second solution was synthesized by silver nitrate dissolved in 100 mL of water while being distilled until silver nitrate dissolved and ammonium hydroxide was added. The silver ion solution that formed was put into a glucose solution in a ratio

of 18. In the solution, PVA was added with a variation of 3% concentration. After that, it was heated at a temperature of 60°C in an Erlenmeyer flask. During the heating process, the mixture is stirred using a magnetic stirrer until it is brown. The brown colloidal silver solution is put into the first solution a little bit and added ammonium hydroxide to a pH of 9 while in the stirrer. Then, it was refluxed for 30 min. after it was filtered and will get a yellow precipitate. It was washed with isopropanol then dried for 5 h at a temperature of 60°C so that yellow powder was obtained. It was calcined at 500°C for 2 h and silver-cerium particles were obtained

### Characterization

The powder X-ray diffractogram of synthesized and calcined samples was recorded on a Rigaku Miniflex diffractometer with  $\text{Cu K}\alpha$  radiation between 1.5 and 10° (2 $\theta$ ) with a scanning rate of 1°/min. TEM micrographs of the samples were obtained with a JEOL 100CX microscope with 100 kV of acceleration voltage. SEM merk JEOL-JSM 6360 LA.

### Antimicrobial activity

The activity test of silver nanoparticles and silver-cerium nanoparticles was carried out follow the AATCC 147-1998 and AATCC standards 100-1999. The type of bacteria used was *Escherichia coli* and *Staphylococcus aureus*. Qualitative or antimicrobial activity testing microbial inhibitory test carried out in a way make a series of dilution test compounds (silver colloidal nanoparticle solution and silver-cerium colloidal nanoparticle solution results synthesis) with a variation of concentration was 25, 50 and 100%. Control was carried out on reagent media test compound. The inhibitory test was carried out with wetting sterile paper discs with nano solution silver the main solution of the silver-cerium nanoparticles colloid produced by the mixture, then put on Petri dishes containing *escherichia coli* test bacteria and *staphylococcus aureus* was grown on Nutrient Agar (NA) and Mueller Hinton Agar (MHA) media. The inhibitory power of the test material was known by measuring the width of the zone of inhibition around the paper discs (in millimeters).

## RESULTS AND DISCUSSION

### XRD analysis

Figure 1 shown the XRD pattern of nanomaterials produced. The appearance of similar

XRD peaks has been observed in JCPDS no. 00-041-1402 data with a hexagonal crystal structure and crystal size ranging from 18.61-30.01 nm for silver nanoparticles. Cerium oxide nanomaterials adjusted to JCPDS data No. 01-073-6318 with a cubic crystal structure with a size of crystal 11.94-27.97 nm. After Ag nanoparticles were doped with cerium oxide a histogram curve was produced which consisted of Ag and Ce peaks. The crystal size of the silver-cerium nanoparticles produced was calculated using the Debye Scherrer equation with the wavelength value,  $2\theta$  and FWHM resulting from the XRD test<sup>13</sup>. From the calculation results obtained the size of crystals 8.9 -12.73 nm. The presence of Ag–O bonds at the interface between the nanoparticles and the supporting oxide ( $\text{CeO}_2$ ) was also detected. The Ag–O interatomic distance decreases with decreasing nanoparticle size<sup>14</sup>. Based on the analysis, silver, cerium and silver-cerium particles with a small size of 100 nm were indeed produced with the nano-sized material. Based on Fig. 1C, it can be shown that several peaks coincide because they are in the same area in position of  $2\theta$ . The complexity of cerium oxide nanoparticles XRD spectrum is probably due to the presence of crystalline organic metallic complex like at  $58, 56^\circ 2\theta$  Fig. 1 A. This smaller crystallite morphology plays important role in biological

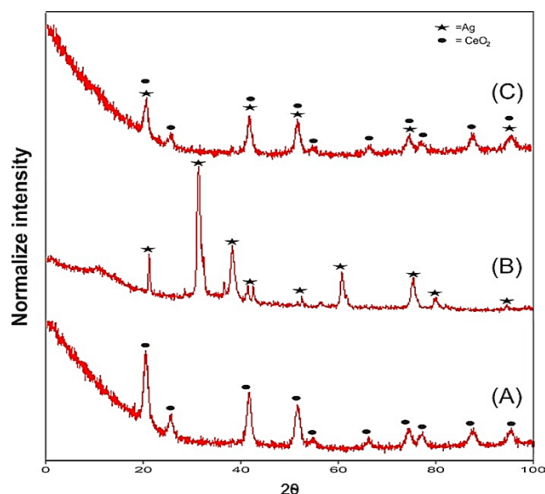


Fig. 1. XRD patterns of (A) silver nanoparticles, (B) cerium oxide nanoparticles and (C) silver-cerium nanoparticles applications of nanostructures<sup>15</sup>.

### TEM Analysis

The results of the TEM images of nanoparticles can be shown in Fig. 2. Fig. 2A and 2B were TEM images of silver nanoparticles and

cerium oxide nanoparticles. They were spherical with uniform size and shape. The measurement results with XRD characterization by using the Debye Scherrer equation to calculate the crystal size. These results were confirmed and strengthened by calculating the particle size of the material produced using image J software image. The results of shown that size of silver cerium nanoparticles ranging from 8.8 to 12.93 nm. Kayama, *et al.*,<sup>16</sup> and Sing, *et al.*,<sup>17</sup> also reported produced silver-cerium nanoparticles

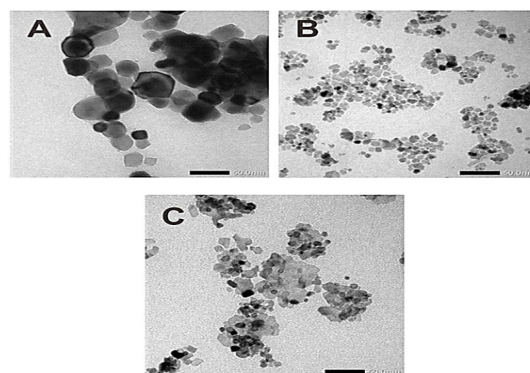


Fig. 2. TEM images of (A) silver nanoparticles (B) cerium oxide nanoparticles and (C) silver-cerium nanoparticles were spherical.

### SEM-EDX

SEM-EDX shown morphological analysis of the material produced. Fig. 3A was an Ag nanoparticle with a uniform particle size. Fig. 3B was a uniform size cerium oxide nanoparticle scattered throughout the surface. Fig. 3C was bimetallic of silver-cerium that was assumed Ag nanoparticles covered by cerium nanoparticles on the surface known as core-shell structured nanoparticles Fig. 3D. Hybrid metal nanoparticles with core-shell structures have advantages such as unique optical properties, high magnetic properties, high electronic properties, and good catalytic properties that

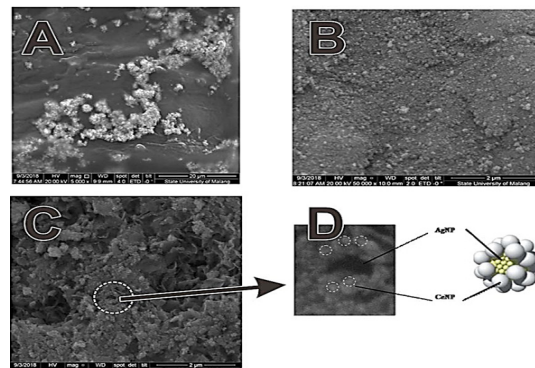


Fig. 3. SEM images of (A) silver nanoparticles (B) cerium oxide nanoparticles (C) silver-cerium nanoparticles and (D) core-shell structures of silver-cerium nanoparticles

monometallic do not have<sup>18</sup>.

However, if the synthesis process was not appropriate, the metal contained in the core cannot interact with the reactants because normally metal oxides found on the surface of the size are relatively large, thus blocking the reaction of the reactants with metals contained in the nucleus<sup>19</sup>. In this research we modified the solvent for the synthesis of the silver-cerium nanoparticles to produce nano-sized cerium nanoparticles, allowing interaction between reactants and metals in the cell nucleus. Based on the results of XRD and TEM analysis, the silver-cerium particles produced have a particle size diameter of 8.9-12.73 nm. The metal in the core can affect the active metal oxides on the surface so as to increase the selectivity

of the bimetal nanoparticles in its application<sup>20</sup>.

Based on the results of the SEM-EDX analysis in Fig. 4, only about 1% of silver metal was present in samples of silver-cerium nanoparticles. This happens because the SEM-EDX analysis was essentially a surface inspection and analysis. The data or appearance obtained was from a surface or layer with a thickness of about 20 micrometers from the surface<sup>21</sup>. Based on Fig. 3D of cerium silver nanoparticles material in the form of core-shell structure where Ag nanoparticles were present in the core and cerium oxide nanoparticles are on the surface so that a large number of cerium oxides appear in the component composition of cerium

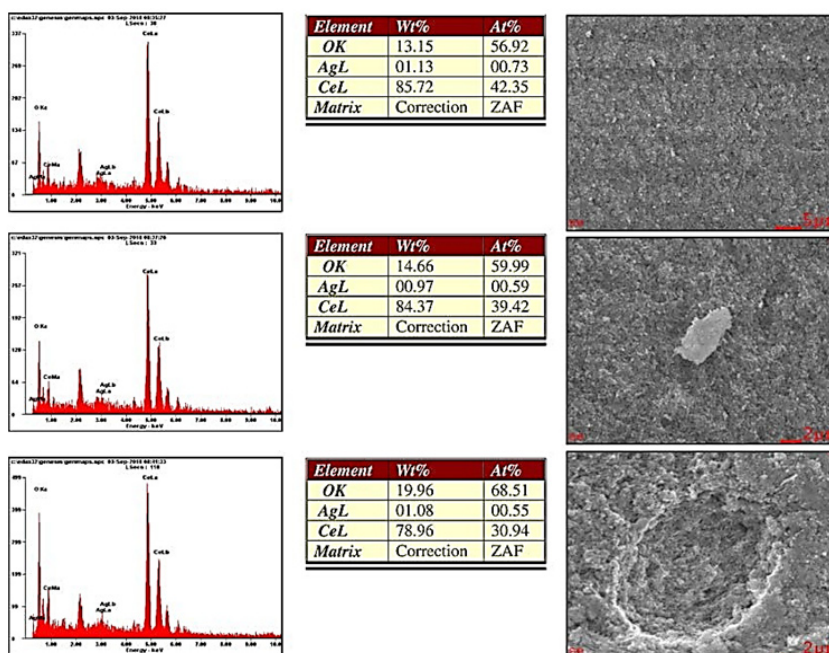


Fig. 4. EDX analysis of silver-cerium nanoparticles

silver nanoparticles.

**Antibacterial activity of silver nanoparticles and silver-cerium nanoparticles**

Antimicrobial activity testing of silver nanoparticles and silver-cerium nanoparticles colloidal solutions in accordance with the standard method of AATCC147-1998<sup>22</sup>. This test is qualitative by measuring how wide the zones of inhibition the media were *Escherichia coli* and *Staphylococcus aureus* that occur after surface contact with paper discs moistened with silver nanoparticle colloid solutions and silver/cerium nanoparticles colloid with variations in concentration was 100, 50, and 25%. Fig. 5 shown that silver nanoparticles

colloid solutions and silver-cerium nanoparticle colloid solutions showed inhibitory activity against *Staphylococcus aureus* (Gram-positive) Fig. A and B and *Escherichia coli* (Gram-negative) Fig. C and D with the formation of zone of inhibition on agar medium containing bacteria even though it had experienced a 25% dilution. The results of this research in accordance with the Sharma *et al.*, 2009 that antibacterial activity of biological synthesized silver nanoparticles was seen against Gram-negative (*Pseudomonas putida* and *Klebsiella pneumonia*, *E. coli*) and (*Staphylococcus aureus* and *Bacillus subtilis*) bacteria. Further, the zone of inhibition of silver nanoparticles against Gram-negative and

*Gram-positive* bacteria were measured. The results indicated that silver nanoparticles synthesized from strawberry leaf extract showed effective antibacterial activity both in *Gram-negative* and *Gram-positive*

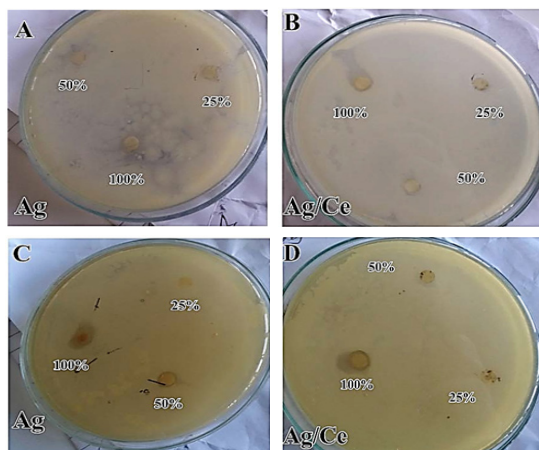


**Fig. 5.** Antibacterial activity of silver nanoparticles (a) and silver-cerium nanoparticles (b) against the growth of *Staphylococcus aureus* bacteria, antibacterial activity of silver nanoparticles (c) and silver-cerium nanoparticles (d) against the growth of *Escherichia coli* bacteria<sup>23</sup>.

The size zone of inhibition showed the

**Table :** The zone of inhibition used Ag and Ag-Ce nanoparticles against bacterial growth

No	Concentration Ag and Ag-Ce nanoparticles solution (%)	Zone of inhibition used Ag nanoparticles		Zone of inhibition used Ag-Ce nanoparticles	
		<i>Staphylococcus aureus</i>	<i>Esherichia coli</i>	<i>Staphylococcus aureus</i>	<i>Esherichia coli</i>
1	control	0	0	0	0
2	25	8.02	0	8.25	6.75
3	50	10.3	8.47	12.6	9.41
4	100	12.5	10.97	17.34	13.52

*E. coli*, although the difference was not wide.

According to Jawetz, *et al.*, (2013) states that antibacterial activity was influenced by 4 factors, namely: extract concentration, a content of metabolite compounds, diffusion power of extract and type of bacteria that are inhibited<sup>26</sup>. Antibacterial inhibitory activity test against *Gram-positive* bacteria (*Bacillus cereus*) was stronger than *Gram-negative* bacteria (*Escherichia coli*) because of the structure of their respective cell walls. Pelczar and Michael (2017), the cell wall structure of *Gram-negative* bacteria is more complex than the cell wall structure of *Gram-positive* bacteria. *Gram-negative* bacteria have cell walls

strength of the nanoparticles inhibitory against bacteria. The wider the zone of inhibition caused showed the stronger the inhibitory power of the compound to bacterial growth<sup>24</sup>. The width of the zone of inhibition formed using silver colloid solution and silver-cerium colloid solution. The resulting zone of inhibition was measured by a calipers run. The results of the measurement of the zone of inhibition Ag and Ag/Ce nanoparticles shown in Tables 1.

Antibacterial activity of silver nanoparticles and silver-cerium nanoparticles on the growth of *Staphylococcus aureus* bacteria shown in Fig. 5A and 5B. The antibacterial activity of silver nanoparticles and silver-cerium nanoparticles on the growth of *Escherichia coli* bacteria shown in Fig. 5C and 5D. The diameter of the zone of inhibition < 5 mm (weak), a zone of inhibition 5-10 mm (medium), a zone of inhibition 10-20 mm (strong) and very strong 20 mm more<sup>25</sup>. Based on Table 1, it had shown the diameter of the zone of inhibition % Ag Colloid Ag solution when 100% in *S. aureus* bacteria 12.5 mm and *E. coli* 10.97 mm. The category of zone inhibition was strong. The disinfection effect of Ag-doped CeONP was more pronounced on *S. aureus* than

which consist of 3 layers, namely, the outer layer, the middle layer, and the inner layer. The function of the outer layer served as a bacterial barrier to the effects of various antibacterials and in the outer layer had membrane porins that function to prevent the entry of other molecules enter into bacteria<sup>27</sup>. Whereas *Gram-positive* bacteria only have a single layer on the cell wall. Siswandono, 2016 added that the relatively complex *Gram-negative* bacterial cell wall structure would cause antibacterial compounds to be more difficult to enter cells and find targets for degradation<sup>28</sup>.

Silver nanoparticles doped with cerium

nanoparticles showed an increase in inhibitory with an increase a zone of inhibition after being doped with cerium nanoparticles because the strong disinfection effect of Ag-doped CeONP was attributed to the synergetic combination of two mechanisms, namely, redox catalysis of surface oxygen vacancy<sup>29</sup>. Ce in comparison to Ag possess two different oxidation states of Ce<sup>3+</sup> (Ce<sub>2</sub>O<sub>3</sub>) and Ce<sup>4+</sup> (CeO<sub>2</sub>) and can tolerate free radicals. Normally, it has been observed that Ce was present in CeO<sub>2</sub> form at CeO<sub>2</sub>-nanoparticles surface having deficient oxygen (O) and valency of Ce<sup>3+</sup> rather than Ce<sup>4+</sup>. This defect chemistry in the surface of pre-activated CeO<sub>2</sub>-nanoparticles can provide the maximum antioxidant potential to them. So, Ce doped Ag can increase the antibacterial activity of nanoparticles<sup>13,30</sup>. Based on Table 1, it had shown the diameter of the zone of inhibition Ag-Ce Colloid solution when 100% in *S. aureus* bacteria 17.34 mm and *E. coli* 13.52 mm. The category of zone inhibition was strong. The

disinfection effect of Ag-doped CeONP was more pronounced on *S. aureus* than *E. coli*, although the difference was not wide.

The zone of inhibition of Ag-Ce was slightly higher than that of nondoped Ce (Table 1) in *E. coli* and *S. aureus*. This finding not only justifies the synergetic effect but also supports the conjecture that Ag-doped Ce-nanoparticles produces more oxygen vacancies such that Ag-doped CeONP disinfects better than a simple combination of ceria particles and silver ions. The disinfection effects of Ag-doped CeONP are also superior to a simple combination of undoped CeONP and equivalent Ag<sup>+</sup> content<sup>31</sup>.

Synthesis nanoparticles using metal oxide reported in the kinds of literature shown in Table 2 and result of this research are found to be comparable to these report. Accordingly, nanoparticles silver doped cerium oxide can be used and potential for

**Table 2: Synthesis nanoparticles using metal oxide**

Nanomaterial Oxide	Size (nm)	Antimycobacterial activity	Ref
Titanium oxide	25,7 – 47,1	Effective antibacterial activity for <i>Staphylococcus aureus</i>	[32]
Copper oxide	23,17	Potential for external uses as antibacterial agents	[33]
Zinc oxide	19.6 -20.2	Antibacterial activity for gram (+ and gram (-)	[34]
Silver oxide	7.0 – 9.0	Lower when tested against <i>E. coli</i> than when tested against <i>S. aureus</i>	[35]
Cerium oxide	20.0 – 100.0	Exhibited inhibition with respect to the gram negative	[36]
Titaniumoxide-Silver	15,0	Higher antibacterial efficacy against <i>E. coli</i> bacteria	[37]
Copper Oxide-Silver	16.0 – 25.0	Excellent antibacterial activity against the growth of microorganisms	[38]
Zinc Oxide-Silver	12-13	Ag-doped ZnO nanoparticles have ability to destroy bacteria and serve as better antimicrobial agent than ZnO	
Silver oxide	18.61 – 30.01	Effective antibacterial activity for <i>S. aureus</i> This work	[39]
Cerium oxide- Silver	8.9 – 12.73	Better antimicrobial agent than AgO This work	

antibacterial effect.

### CONCLUSION

The aim of this research was to made agen antibacteri from silver nanoparticles and silver-cerium nanoparticles. XRD and TEM analysis showed silver-cerium nanoparticles were spherical with the dominant size range of 8.9-12.73 nm. SEM-EDX analysis showed silver nanoparticles covered by silver nanoparticles that were known as the core-shell structure. Silver nanoparticles doped the Grant No. 22/INS-1/PPK/E4/2018.

### REFERENCES

- Colussi, S.; Trovarelli, A.; Cristiani, C.; Lietti, L.; Groppi, G. *Catal. Today.*, **2012**, *180*, 124-130.
- Maqbool, Q.; Nazar, M.; Naz. S.; Hussain, T;

with cerium nanoparticles showed an increase in inhibitory with an increase a zone of inhibition after being doped with cerium nanoparticles.

### ACKNOWLEDGEMENT

The authors would like to Government of Indonesia by Direktorat Jendral Penelitian dan Pengabdian Masyarakat (DRPM) Riset Teknologi dan Pendidikan Tinggi (Ristekdikti), through research schemes Insentif Riset Sistem Inovasi Nasional (Insinas) for providing funds of this research with

- Jabeen,N.; Kausar, R.; Anwaar, S.; Abbas, F.; Jan, T. *Int. J. Nanomed.*, **2016**, *11*, 5015-5025.
- Cresi, J.S.; Spadaro, M.C.; D'Addato, S.; Valeri, S.; Amidani, L.; Boscherini, F.; Bertoni, G.; Deiana, D.;

4. Luches, P. *Nanotechnology.*, **2017**, *28*, 49.
5. Shimizu, K.; Kawachi, H.; Satsuma, A. *Appl. Catal.B: Environ.*, **2010**, *96*,167-175.
6. Choi, H.W.; Lee, K.H.; Hur, N.H.; Lim, H.B. *Anal.Chim.Acta.*, **2014**, *847*, 10-15.
7. Bing, J.; Li, L.; Lan, B.; Liao, G.; Zeng, J.; Zhang, Q.; Li, X. *Appl.Catal.B: Environ.*, **2012**, *115*, 16.
8. Putri, G.E.; Arief, A.; Jamarun, N.; Gusti, F.R.; Fisi, A. Zilfa, Septiani, U. *J. Applicable.Chem.*, **2017**, *6*, 1058-1068.
9. Vargas, G.O.A; De los Rayes Heredia, J.A.; Montesinos Castellanos, A.; Chen, L.F.; Wang, J.A. *Mater. Chem. Phys.*, **2013**, *139*, 125.
10. Jabbar, S.S. *Orient. J. Chem.*, **2018**, *34*, 2026-2030.
11. Naik, B.; Hazra, S.; Prasad, V.S.; Ghosh, N.N. *Catal. Commun.*, **2012**, *12*, 1104.
12. Chaiyasat, A.; Jearani, S.; Moonmangmee, S.; Moonmangmee, D.; Christopher, L.P.; Alam, M.N.; Chaiyasat, P. *Orient. J. Chem.*, **2018**, *34*, 1735-1740.
13. Wang, L.; He, H.; Yu, Y.; Sun, L.; Liu, S.; Zhang, C.; He, L. *J. Inorg. Biochem.*, **2014**, *135*, 45.
14. Maqbool, Q. *RSC Adv.*, **2017**, *7*, 56575.
15. Benedetti, F.; Luches, P.; Spadaro, M.C.; Gasperi, G.; D'Addato, S.; Valeri, S.; Boscherini, F. *J. Phys. Chem.*, **2015**, *119*, 6024-6032.
16. Khadar, Y.A.; Balamurugan, A.; Devarajan, V.P.; Subramanian, R. *Orient. J. Chem.*, **2017**, *33*, 2405-2411.
17. Kayama, T.; Yamazaki, K.; Shinjoh, H. *J. Am. Chem. Soc.*, **2010**, *132*, 13154.
18. Singh, G.; Joyce, M.A.; Beddow, J.; Timothy, J.; Mason, J. *J. Microbio. Biotech. Food Sci.*, **2012**, *2*, 106.
19. Mitsudome, T.; Mikami, Y.; Matoba, M.; Mizugaki, T.; Jitsukawa, K.; Kaneda, K. *Angew. Chem. Int. Ed.*, **2012**, *51*, 136.
20. Strasser, P.; Koh, S.; Anniyev, T.; Greeley, J.; More, K.; Yu, C.F.; Liu, Z.C.; Kaya, S.; Nordlund, D.; Ogasawara, H.; Toney, M.F.; Nilsson, A. *Nat. Chem.*, **2010**, *2*, 454.
21. Ghorbani, H.R. *Orient. J. Chem.*, **2014**, *30*, 1941-1949.
22. Sen, P.; Ghosh, J.; Abdullah, A.; Kumar, P. Vanada. *Proc. Indian Acad.Sci.(Chem. Sci.)*, **2003**, *115*, 499-508.
23. Singh, H.; Du, J.; Yi, T.H. *Artif. Cells Nanomed. Biotech.*, **2017**, *45*, 1310.
24. Sharma, V.K.; Yngard, R.A.; Lin, Y. *Adv Colloid Interface Sci.*, **2009**, *145*, 83-96.
25. Shin, S.H.; Kim, Y.H.; Park, W.K.; Jung, H.C.; Koo, K.W.; Kim; Sook. *Appl. Environ. Microbiol.*, **2008**, *74*, 2171.
26. Davis, W.W and Stout, T.R. *Appl Microbiol.*, **1971**, *22*, 659-665.
27. Jawetz, Melnick, Adelberg's. *Medical Microbiology*. Twenty-Sixth Edition. Geo. F. Brooks, MD. Professor of Laboratory Medicine. a LANGE Medical Book., **2013**.
28. Pelczar, Michael, J. *Microbio.*, 7<sup>th</sup> edition, McGraw-Hill Companies, New York., **2017**.
29. Siswandono. *Kimia Medisinal*, Airlangga University Press. Indonesia., **2016**, *2*.
30. Feng, Q.L.; Wu,.; Chen, G.Q.; Cui, F.Z.; Kim, T.N.; Kim, J.O. *J. Biomed. Mater. Res.*, **2000**, *52*, 662-6688.
31. Bae, E.; Park, H.J.; Park, j.; Yoon, J.; Kim, Y.; Choi, K.; Yi, J. *Bull. Korean Chem. Soc.*, **2011**, *32*, 613-619.
32. Tsai, D.S.; Yang, T.S.; Huang, Y.S.; Peng, P.W.; Ou, K.L. *Inter.J. Nanomed.*, **2016**, *1*, 2531-2542.
33. Xing, Y.; Li, X.; Zhang, L.; Xu, Q.; Che, Z.; Li, W.; Bai, Y.; Li, K. *Progr.Organic Coat.*, **2012**, *73*, 219-224.
34. Ahamed, M.; Alhadlaq, H.A.; Khan, M.A.A.; Karuppiyah, P.; Al-Dhabi, N.A. *J. Nanomater.*, **2014**, *637858*, 4.
35. Shahid, S.; Khan, S.A.; Ahmad, W.; Fatima, W.; Knawal, S.; *Indian J.Pharm Sci.*, **2018**, *80*,173-180.
36. Kim, J.S.; Kuk, E.; Yu, K.N.; Kim, J.; Park, S.J.; Lee, H.J.; Kim, S.H.; Park, Y.K.; Park, Y.H.; Hwang, C.; Kim, Y.; Lee, Y.; Jeong, D.H.; Cho, M. *Nanomed. Nanotech. Bio. Med.*, **2014**, *10*, 1119.
37. P. Reshma, K. Ashwini. *J Nanomater Mol Nanotechnol.*, **2017**, *6*, 3.
38. Thiel, J.; Pakstis, L.; Buzby, S.; Raffi, M.; Ni, C.; Pochan, D.J.; Ismat Shah, S. *Small Journal.*, **2017**, *3*, 799-803.
39. Sasikala, R.; Kutti Rani, S; Karthikeyan, K.; Easwaramoorthy, D. *DJ J. Eng. Chem. Fuel.*, **2016**, *1*, 43-51.
40. Dowlatabadi, F.H.; Amiri, A.; Sichani, M. M.